Cell Reports
Report

Activated CaMKII Couples GluN2B and Casein Kinase 2 to Control Synaptic NMDA Receptors

Antonio Sanz-Clemente,[1] John A. Gray,[2] Kyle A. Ogilvie,[1] Roger A. Nicoll,[2,3] and Katherine W. Roche[1,*]
[1]Receptor Biology Section, National Institute of Neurological Disorders and Stroke (NINDS), National Institutes of Health, Bethesda, MD 20892, USA
[2]Department of Cellular and Molecular Pharmacology
[3]Department of Physiology
University of California, San Francisco, CA 94143, USA
*Correspondence: rochek@ninds.nih.gov
http://dx.doi.org/10.1016/j.celrep.2013.02.011

SUMMARY

Synaptic activity triggers a profound reorganization of the molecular composition of excitatory synapses. For example, NMDA receptors are removed from synapses in an activity- and calcium-dependent manner, via casein kinase 2 (CK2) phosphorylation of the PDZ ligand of the GluN2B subunit (S1480). However, how synaptic activity drives this process remains unclear because CK2 is a constitutively active kinase, which is not directly regulated by calcium. We show here that activated CaMKII couples GluN2B and CK2 to form a trimolecular complex and increases CK2-mediated phosphorylation of GluN2B S1480. In addition, a GluN2B mutant, which contains an insert to mimic the GluN2A sequence and cannot bind to CaMKII, displays reduced S1480 phosphorylation and increased surface expression. We find that although disrupting GluN2B/CaMKII binding reduces synapse number, it increases synaptic-GluN2B content. Therefore, the GluN2B/CaMKII association controls synapse density and PSD composition in an activity-dependent manner, including recruitment of CK2 for the removal of GluN2B from synapses.

INTRODUCTION

The molecular composition of the postsynaptic density (PSD) at excitatory synapses is profoundly modified in response to synaptic activity, including changes in receptors, scaffolding proteins, and signaling enzymes (Ehlers, 2003). Glutamate receptors are important constituents of PSDs, and the dynamic regulation of their synaptic expression is a central mechanism for modulating the strength of excitatory neurotransmission. Therefore, glutamate receptors are subject to strict controlling mechanisms that allow both short- and long-term modifications in their number, localization, and composition in a cell- and synapse-specific manner (Traynelis et al., 2010). N-methyl-D-aspartate receptors (NMDARs) are ionotropic glutamate receptors, which, after activation, allow calcium influx into the postsynaptic spine and trigger a variety of intracellular signaling cascades (Lau and Zukin, 2007; Sanz-Clemente et al., 2013). Synaptic NMDARs are dynamically regulated. For example, there is a switch in the synaptic composition of NMDARs during development, from GluN2B-containing to GluN2A-containing receptors (Carmignoto and Vicini, 1992; Quinlan et al., 1999). Although several molecular mechanisms, including phosphorylation and protein-protein interactions, have been identified for controlling NMDAR subcellular localization and trafficking, our understanding of synaptic NMDAR regulation remains incomplete (Groc et al., 2009; Sanz-Clemente et al., 2013).

We have recently reported that casein kinase 2 (CK2) regulates subunit composition of synaptic NMDARs by driving the removal of GluN2B from the synapse. CK2 phosphorylation of the PDZ ligand of GluN2B (S1480) disrupts the interaction of GluN2B with scaffolding proteins and allows the lateral diffusion of the receptor out of the synapse (Chung et al., 2004; Sanz-Clemente et al., 2010). CK2 is a constitutively active kinase, which is not directly regulated by calcium (Hathaway and Traugh, 1982; Olsten and Litchfield, 2004). The CK2-mediated phosphorylation of GluN2B S1480, however, requires calcium influx through NMDARs (Chung et al., 2004; Sanz-Clemente et al., 2010). Thus, it remains unclear how the NMDAR-mediated increase in postsynaptic calcium regulates NMDARs via phosphorylation of GluN2B S1480 by CK2.

CaMKII is a major component of the PSD and it is known that CaMKII translocates to synapses in an activity-dependent manner to interact with GluN2B-containing NMDARs (Coultrap and Bayer, 2012; Merrill et al., 2005). We report here an unexpected structural role for the activity-dependent association of GluN2B and CaMKII in regulating synaptic NMDARs by coupling CK2 to the receptor and facilitating the phosphorylation of GluN2B within its PDZ ligand. Specifically, we show that CK2 binds to GluN2B upon CaMKII association with the receptor. Consequently, activated CaMKII promotes the CK2-mediated phosphorylation of the PDZ ligand of GluN2B (S1480) to control the synaptic expression of NMDARs.

RESULTS

The phosphorylation of GluN2B by CK2 within its PDZ ligand (S1480) (Figure 1A) is promoted by NMDAR activity, and the pharmacological blockade of CaMKII results in the attenuation

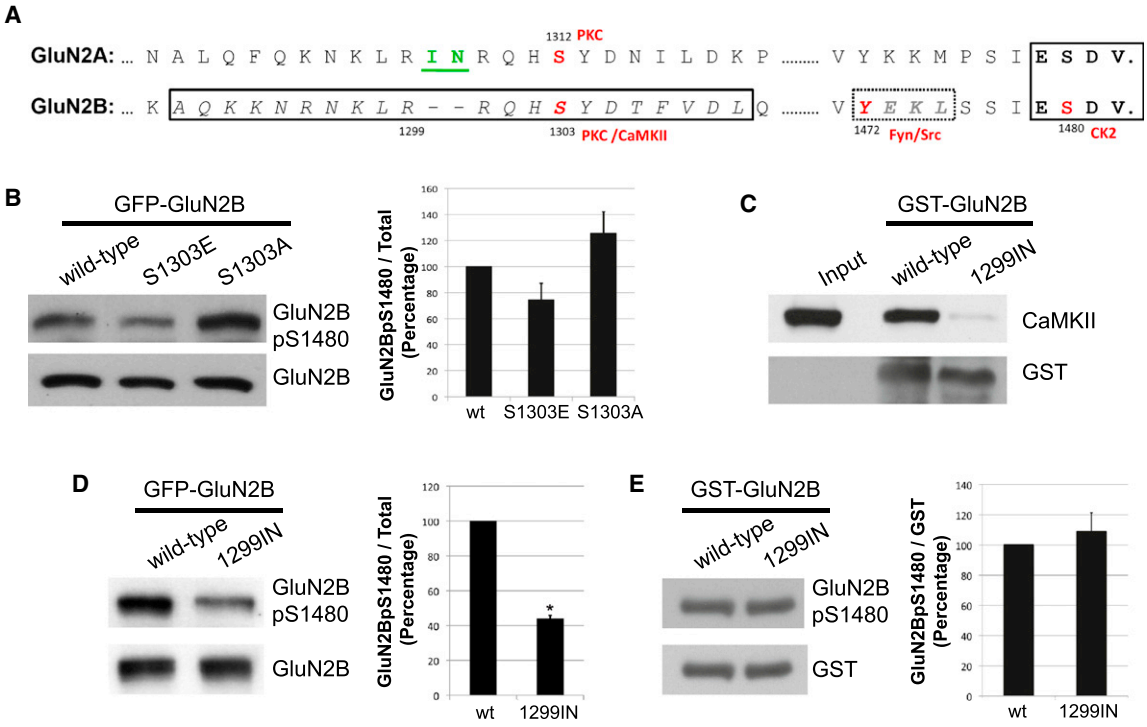

Figure 1. Disruption of the CaMKII Binding Site on GluN2B Results in a Decrease in GluN2B S1480 Phosphorylation

(A) Alignment of rat GluN2A and GluN2B subunits, showing the CaMKII binding site (italics boxed) and the YEKL endocytic motif (dotted boxed) on GluN2B. The PDZ ligand is shown in bold, and residues in red are phosphorylated by the indicated kinases. The two residues (IN) inserted in GluN2B to mimic the GluN2A sequence are shown underlined in green.

(B) HEK293T cells were transfected with GluN1, PSD-95, and GluN2B (WT or mutants), and the level of GluN2B S1480 phosphorylation was analyzed by immunoblotting. Graph represents mean ±SEM, n = 4.

(C) Pull-down experiment of GST-GluN2B (WT or 1299IN). Beads were incubated with lysate of HEK293T cells expressing WT CaMKII in the presence of 1 mM $CaCl_2$ and 3 μM calmodulin (Ca^{2+}/CaM), and the bound proteins were analyzed with the indicated antibodies.

(D) GluN2B S1480 phosphorylation was analyzed by immunoblotting after transfection into HEK293 cells as explained in (B). Graph represents mean ±SEM. *$p < 0.05$ in a Wilcoxon test. n = 5.

(E) In vitro phosphorylation of GluN2B (aa 1120–1482) by CK2. GST-GluN2B WT or 1299IN were incubated with CK2 and ATP for 30 min at 30°C. Level of S1480 phosphorylation was analyzed by immunoblotting using a specific phospho-state antibody.

See also Figure S1.

of GluN2B S1480 phosphorylation (Chung et al., 2004; Sanz-Clemente et al., 2010) (Figures S1A and S1B). In addition, it has been reported that CaMKII directly phosphorylates GluN2B on S1303 (Omkumar et al., 1996). Therefore, we investigated if CaMKII-mediated phosphorylation of GluN2B S1303 promotes CK2 phosphorylation (on S1480), perhaps by inducing a favorable conformational change in the GluN2B C-tail. To test this hypothesis, we generated two GluN2B mutants to either mimic or block phosphorylation of S1303 (S1303E or S1303A, respectively) and analyzed their level of S1480 phosphorylation by immunoblotting after transfection into HEK293T cells. We found that GluN2B S1303E did not enhance S1480 phosphorylation. In fact, the CK2 phosphorylation appeared to be diminished, although the effect was not statistically significant (Figure 1B).

This result led us to investigate a second potential mechanism that might regulate the interplay between CK2 phosphorylation of GluN2B S1480 and activation of CaMKII: the physical binding of CaMKII to GluN2B (residues 1290–1309) (Figure 1A) (Bayer et al., 2001; Strack et al., 2000). Importantly, it has been shown that phosphorylation of GluN2B S1303 reduces GluN2B/CaMKII binding (O'Leary et al., 2011; Strack et al., 2000). Because GluN2A does not interact with CaMKII in this region (Strack et al., 2000), we generated a GluN2B mutant in which two residues (IN) were inserted after R1299 (GluN2B 1299IN), to mimic the GluN2A sequence in the analogous region (Figure 1A). Using a pull-down assay, we found that GluN2B 1299IN does not bind to CaMKII (Figure 1C). We next analyzed the levels of CK2 phosphorylation of the PDZ ligand of GluN2B wild-type (WT) or 1299IN. Notably, the phosphorylation of GluN2B 1299IN on S1480 was dramatically reduced (Figure 1D). However, CK2 phosphorylation of GluN2B 1299IN and WT on S1480 was indistinguishable in an in vitro phosphorylation assay (Figure 1E), suggesting that the direct interaction between GluN2B and CaMKII promotes S1480 phosphorylation in situ (Figure 1D), but the mutations per se do not alter CK2 phosphorylation of S1480.

We have recently reported that GluN2B S1480 phosphorylation decreases receptor surface expression by disrupting GluN2B binding with MAGUK proteins and inducing

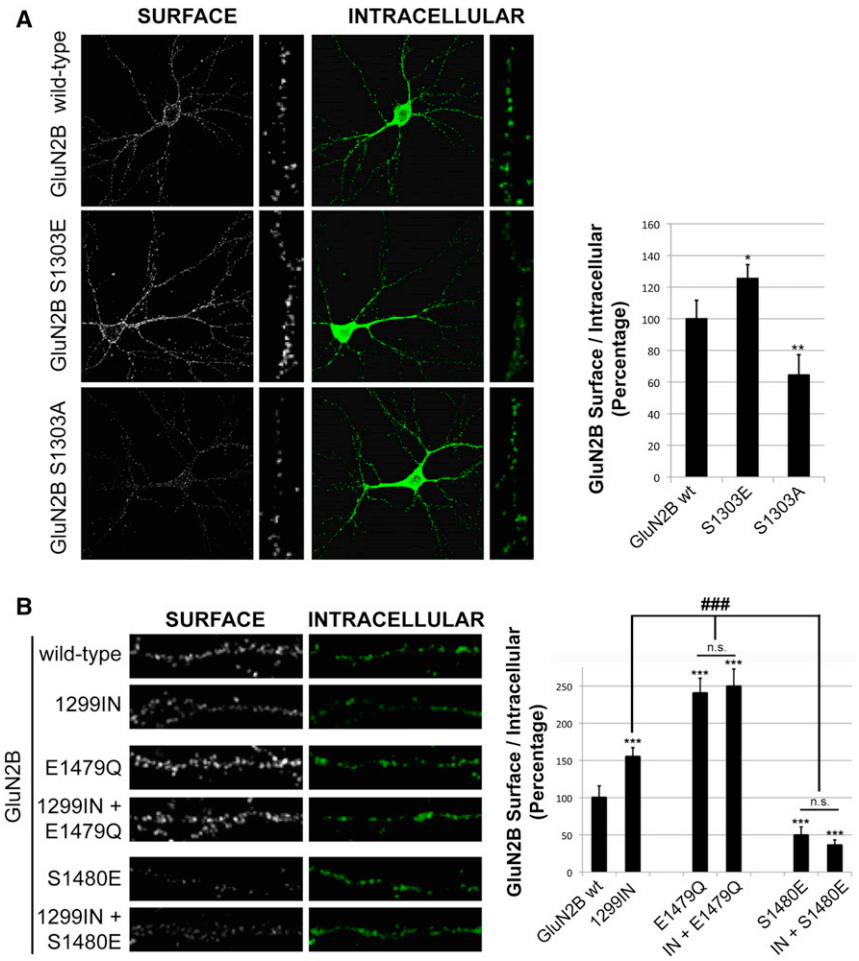

Figure 2. Disruption of the GluN2B/CaMKII Association Increases the Surface Expression of GluN2B via S1480 Phosphorylation

(A and B) Hippocampal neurons were transfected at DIV7 with GFP-GluN2B WT or mutants. At DIV11–12, surface-expressed receptors were labeled with GFP antibody and Alexa-555-conjugated secondary antibody (shown in white). After permeabilization, the internal pool of receptors was visualized by anti-GFP and Alexa-633-conjugated antibody (green). Graph represents means ±SEM. $^{**}p < 0.01$, $^{***}p < 0.001$ in a one-way ANOVA test; n (WT, S1303E, S1303A) = 27, 30, 24 (A); n (WT, IN, E1479Q, IN+E1479Q, S1480E, IN+S1480E) = 23, 29, 22, 19, 20, 28 (B).

Data are from four independent experiments.

internalization (Sanz-Clemente et al., 2010). Therefore, we tested whether the GluN2B/CaMKII association controls GluN2B surface expression. GFP-tagged GluN2B mutants were expressed in dissociated hippocampal cultures, and surface-expressed receptors were visualized by confocal microscopy. We found that impairing CaMKII binding to GluN2B receptors with either the S1303E (Figure 2A) or the 1299IN (Figure 2B) mutations resulted in increased surface expression. In contrast, GluN2B S1303A was less efficiently expressed on the cell surface (Figure 2A). To test if the GluN2B/CaMKII association regulates GluN2B surface expression via S1480 phosphorylation, we generated GluN2B mutants containing both a disrupted CaMKII binding site (1299IN) and altered S1480 phosphorylation (phospho-mimetic: S1480E; and phospho-deficient: E1479Q) (Sanz-Clemente et al., 2010). Importantly, we found that the mutations in the PDZ ligand, S1480E or E1479Q, occluded the effect of GluN2B/CaMKII association in controlling GluN2B surface expression (Figure 2B), suggesting a common molecular mechanism to control GluN2B surface expression and that GluN2B/CaMKII binding is an event occurring upstream of CK2 phosphorylation.

Although CK2 is a constitutively active kinase, the phosphorylation of its substrates can be regulated by several mechanisms, including CK2 localization and targeting to specific structures via specific protein-protein interactions (Litchfield, 2003). Thus, we tested if CaMKII binding to GluN2B facilitates the association of CK2 with GluN2B. We first isolated GluN2B-containing protein complexes from cultured cortical neurons using a specific GluN2B antibody and found that CaMKII coimmunoprecipitated with GluN2B and, importantly, CK2 was also found in the same protein complex (Figure 3A). The AMPA receptor subunit GluA2, evaluated as a negative control, did not coimmunoprecipitate with GluN2B, indicating the specificity of our assay. To determine whether the GluN2B/CaMKII interaction is essential for CK2 binding to GluN2B, we carried out pull-down assays incubating GST-GluN2B (WT or 1299IN) with cell lysate from HEK293T cells expressing CaMKII. Because the binding of CaMKII to GluN2B (residues 1290–1309) is calcium dependent (Bayer et al., 2001), we performed these experiments in the presence of calcium and calmodulin (CaM) or EGTA (as a negative control). We found that both CaMKII and CK2 associate with GluN2B WT in the presence of Ca^{2+}/CaM, but, strikingly, CK2 does not bind to GluN2B 1299IN, which is unable to bind to CaMKII (Figure 3B). Importantly, neither CaMKII nor CK2 interact with GluN2B in the presence of EGTA. As expected, both GluN2B WT and 1299IN bind to PSD-95, evaluated as a control.

Two other GluN2B mutants with impaired binding to CaMKII have been characterized (Barria and Malinow, 2005; Halt et al., 2012) (Figure 3C). Therefore, we also tested the CK2 association to these GluN2B mutants and found that, similar to GluN2B 1299IN, they failed to precipitate CK2 in a pull-down assay performed in the presence of Ca^{2+}/CaM (Figure 3D).

Our data support the existence of a trimolecular GluN2B/CaMKII/CK2 complex. To test for direct interaction between the two kinases, CaMKII and CK2, we performed pull-down experiments, by incubating GST-CK2 with CaMKII (WT or T286D) in the presence of Ca^{2+}/CaM or EGTA. We observed a robust

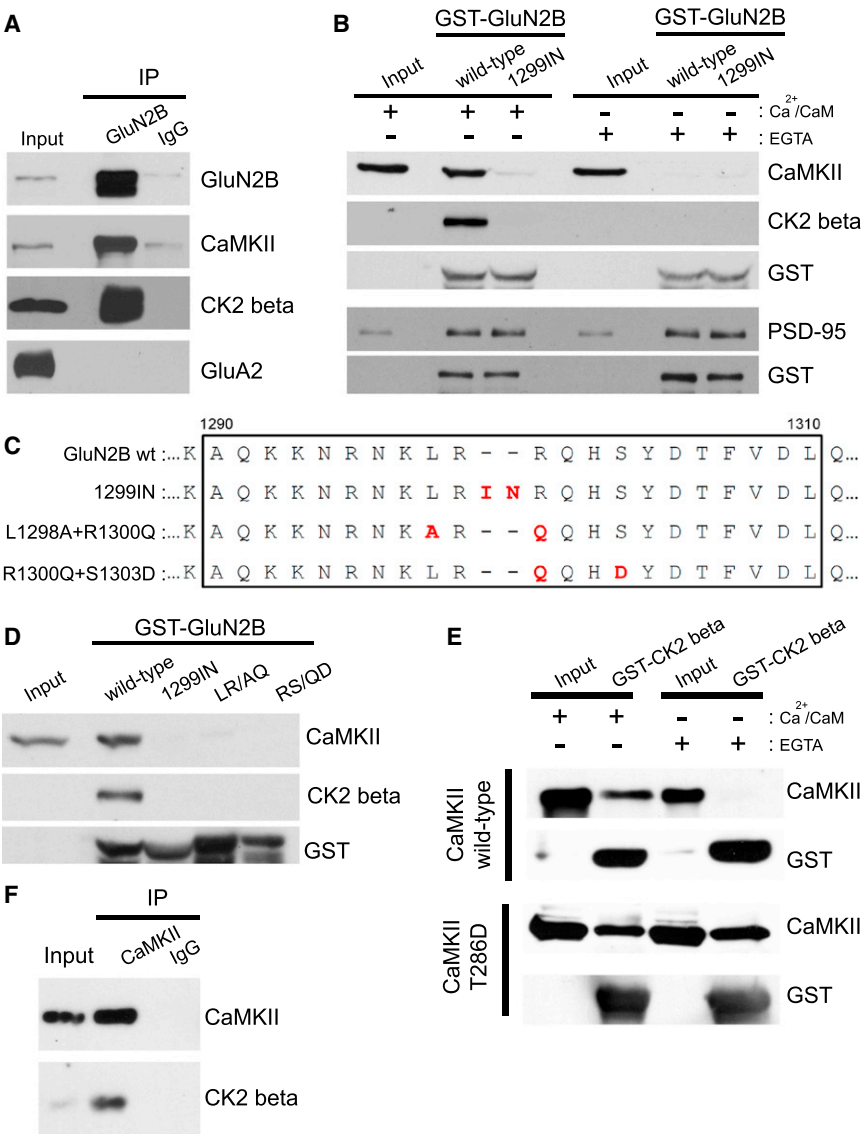

Figure 3. Activated CaMKII Binds to CK2 and Promotes the Coupling of CK2 to GluN2B

(A) The P2 fraction from cortical cultures (DIV15) was isolated, and, after lysis, the association of CaMKII and CK2 to GluN2B was analyzed by immunoprecipitation with anti-GluN2B antibody.

(B) Pull-down experiments of GST-GluN2B (WT or 1299IN) performed as in Figure 1C. Beads were incubated with lysate of HEK293T cells expressing WT CaMKII (or PSD-95 as a control) in the presence of 1 mM $CaCl_2$, 3 μM calmodulin (Ca^{2+}/CaM), or 1 mM EGTA (EGTA), and the bound proteins were analyzed with the indicated antibodies.

(C) Sequence of GluN2B and several GluN2B mutants with impaired CaMKII association (Barria and Malinow, 2005; Halt et al., 2012). The mutated residues are shown in red, and the CaMKII binding site is boxed.

(D) A pull-down assay was performed with the GluN2B mutants showed in (C) as described in (B), including Ca^{2+}/CaM. Bound proteins were analyzed by SDS-PAGE and immunoblotted with the indicated antibodies.

(E) Pull-down experiments performed as in (B). GST-CK2 beta was incubated with lysate of HEK293T expressing WT CaMKII or T286D.

(F) Lysate of HEK293 cells expressing CaMKII T286D was incubated with anti-CaMKII antibody, and, after washes, the recovered material was blotted with the indicated antibodies.

interaction between the two kinases when CaMKII is activated (Figure 3E). Similarly, endogenous CK2 was coimmunoprecipitated from CaMKII-expressing HEK293T cell lysate using a CaMKII-specific antibody (Figure 3F). Together, these data show that activated CaMKII interacts with CK2, supporting a model in which the binding of CaMKII to GluN2B results in the targeting of CK2 to NMDARs.

To physiologically assess the effects of GluN2B mutations on the synaptic localization of NMDARs, we analyzed NMDAR-mediated excitatory postsynaptic currents (EPSCs) in biolistically transfected organotypic hippocampal slice cultures. However, it has been recently reported that the GluN2B/CaMKII association is critical for maintenance of synapse density (Gambrill and Barria, 2011). We examined our mutation GluN2B 1299IN, which disrupts binding to CaMKII, and analyzed synapse number by measuring the colocalization of endogenous pre- and postsynaptic markers (VGlut1 and PSD-95, respectively) (Ippolito and Eroglu, 2010). As shown in Figure 4A, we found that expression of GluN2B 1299IN in hippocampal cultured neurons drives a reduction in the number of synapses compared with WT GluN2B, consistent with previous reports (Gambrill and Barria, 2011; Pi et al., 2010). Therefore, we anticipated the role of GluN2B/CaMKII binding on GluN2B trafficking might be obscured by changes in synapse number when analyzing the amplitude of NMDAR currents. However, given the differential decay properties of the GluN2 subunits (Cull-Candy and Leszkiewicz, 2004), the analysis of NMDAR kinetics is a powerful and reliable method to compare the relative contributions of synaptic GluN2A- and GluN2B-containing NMDARs.

Thus, to evaluate the effects of disrupting the GluN2B/CaMKII association on synaptic NMDAR currents (NMDAR-EPSCs), we utilized a molecular replacement strategy in hippocampal slice cultures from GluN2B conditional knockout mice (*Grin2b*$^{fl/fl}$). Slices were biolistically transfected with Cre recombinase and GluN2B constructs (WT or 1299IN) at days in vitro (DIV)2–DIV4, and then simultaneous dual whole-cell recordings were obtained from a transfected neuron and a neighboring nontransfected control cell at DIV18–24. Transfection of Cre alone reduced the NMDAR-EPSC by approximately 40%, consistent with our previous report in acute hippocampal slices (Gray et al., 2011), and, as expected, the EPSC decay was significantly faster,

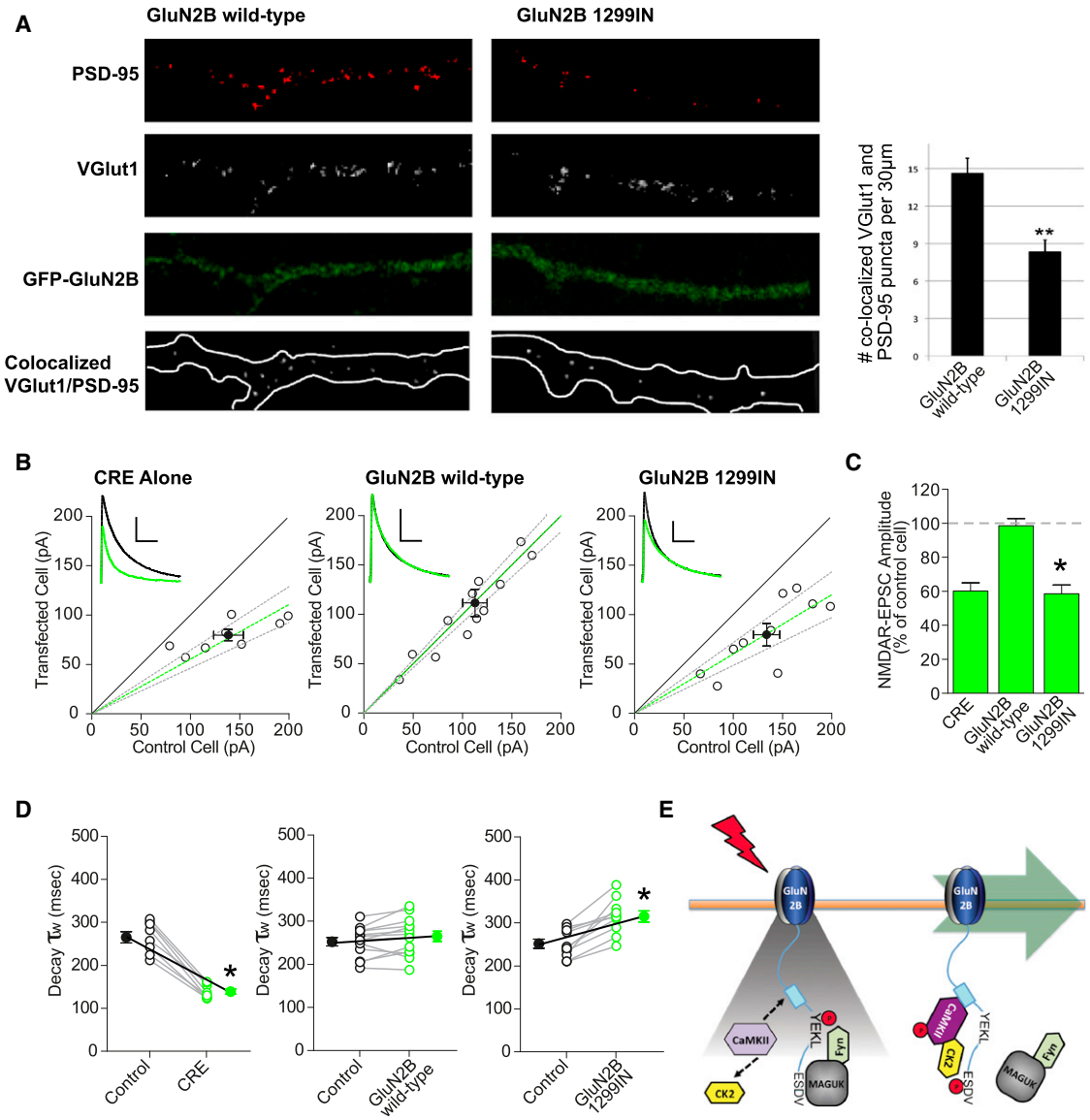

Figure 4. Disrupting the GluN2B-CaMKII Interaction Increases Synaptic Localization of GluN2B-Containing NMDARs

(A) (upper) Cultured hippocampal neurons were transfected with WT GFP-GluN2B or 1299IN at DIV5 and endogenous PSD-95 (red) and VGlut1 (white) labeled at DIV17. (lower) Synapses were identified by colocalization of PSD-95 and VGlut1 in transfected neurons and quantified. Graph represents mean of colocalized puncta per 30 µm ± SEM. **p < 0.01 in a Student's t test; n (WT, 1299IN) = 33, 32. Data are from three independent experiments.

(B and C) Organotypic hippocampal slice cultures were made from P7 *Grin2b*$^{fl/fl}$ mice, biolistically transfected on DIV2–4, and paired whole-cell recordings were obtained from Cre-expressing and neighboring CA1 pyramidal neurons on DIV18–24. (B) Scatterplots of peak amplitudes of NMDAR-EPSCs from single pairs (open circles) and mean ± SEM (filled circles) from transfected and control cells (mean amplitude (pA): left, Cre alone, control 138.6 ± 15.0, transfected 79.7 ± 5.7, n = 8; center, GluN2B WT, control 112.7 ± 12.4, transfected 111.6 ± 13.9, n = 13; right, GluN2B 1299IN control 133.9 ± 13.5, transfected 79.7 ± 11.5, n = 10). Dashed lines represent linear regression and 95% confidence interval. Sample traces are as follows: control cell, black; transfected cell, green; scale bars represent 300 ms and 50 pA. (C) Summary graph of NMDAR-EPSC amplitudes. Bars represent the mean ±SEM of the ratios of transfected to control cells from each pair, expressed as percentages (Cre alone 60.2 ± 4.8, n = 8; GluN2B WT 98.6 ± 4.2, n = 13; GluN2B 1299IN 58.6 ± 5.3, n = 10).

(D) NMDAR-EPSC decay times from cell pairs expressed in ms as a weighted tau (τ_w) from paired transfected and control cells (mean decay, ms: left, Cre alone, control 264.5 ± 12.0, transfected 139.5 ± 5.9, n = 8, p < 0.0001; center, GluN2B WT, control 253.0 ± 9.7, transfected 256.5 ± 12.4, n = 13, p = 0.57; right, GluN2B 1299IN, control 251.4 ± 10.5, transfected 315.5 ± 13.3, n = 10, p < 0.0001). Decay kinetics were analyzed by a paired Student's t test, *p < 0.0001.

(E) Model for the role of GluN2B/CaMKII association in controlling synaptic GluN2B-containing NMDARs. Synaptic activity increases calcium concentration in spines (via NMDARs) and activates CaMKII. Activated CaMKII associates with both GluN2B and CK2 generating a trimolecular complex GluN2B/CaMKII/CK2. CK2 phosphorylation on GluN2B S1480 is promoted by the close proximity of the kinase, which disrupts the interaction between GluN2B and MAGUK proteins and promotes lateral diffusion of GluN2B to extrasynaptic sites.

See also Figure S2.

suggesting removal of endogenous GluN2B (Figures 4B–4D, left). Importantly, replacement with WT GluN2B fully and precisely recovered both the amplitude and decay of the NMDAR-EPSCs (Figures 4B–4D, center). Consistent with a decrease in synapse number, GluN2B 1299IN expression did not fully recover the NMDAR-EPSC amplitude but, importantly, did significantly slow the decay kinetics (Figures 4B–4D, right). The slower decay observed with GluN2B 1299IN expression is consistent with an increased contribution of GluN2B-containing NMDARs at synapses when the CaMKII interaction is disrupted. Similar results were obtained with GluN2B 1299IN overexpression in WT hippocampal slices, though there was less NMDAR-EPSC amplitude loss, likely due to some retained CaMKII interaction with endogenous GluN2B subunits (Figure S2A).

To confirm that the slower NMDAR-EPSC decay with GluN2B 1299IN is not due to receptor gating effects, we expressed WT and mutant GluN2B on a GluN2-null background as previously described (Chen et al., 2012) We find that the decay kinetics of a pure population of GluN2B 1299IN-containing NMDARs is not significantly different from a pure WT GluN2B population (Figure S2B). Again, the peak amplitude of the NMDAR-EPSC from the GluN2B 1299IN expressing neurons is significantly reduced, consistent with a loss of synapses (Figure S2B).

DISCUSSION

In this study, we identify a role for CaMKII in controlling synaptic NMDAR composition. Specifically, we show that GluN2B mutants with impaired binding to CaMKII display a reduction in the CK2-mediated phosphorylation of the GluN2B PDZ ligand, and a concomitant increase in receptor synaptic expression. Remarkably, we have identified an association of CK2 and GluN2B upon CaMKII binding to the receptor. These observations support a model in which the binding of activated CaMKII to GluN2B couples CK2 to the receptor and, therefore, facilitates the phosphorylation of GluN2B S1480 within its PDZ binding domain (Figure 4E).

CK2 is a ubiquitous serine/threonine kinase, although its activity in brain, especially in cortex and hippocampus, is higher than in other nonneuronal tissues (Blanquet, 2000). Typically, CK2 exists as a tetramer composed of two catalytic subunits (alpha or alpha prime) and two regulatory subunits (beta). CK2 is considered to be constitutively active. However, a number of mechanisms regulate CK2 in vivo, including control of CK2 expression level, assembly, and stability and phosphorylation of either alpha or beta CK2 subunits (Litchfield, 2003). Another reported mode of modulating phosphorylation by CK2 is the targeting of the kinase to specific structures. Examples of this regulatory mechanism are the binding of CK2 to tubulin, FAF-1, or CKIP-1 (Litchfield, 2003). We have now identified an unexpected interaction between activated CaMKII and CK2 that supports a role for CaMKII as a scaffolding protein to couple CK2 to synaptic GluN2B and promote GluN2B removal from synapses.

CaMKII is a large holoenzyme composed of 12 subunits, which is activated by calcium influx to the synapse (mainly via NMDARs) and phosphorylates many synaptic substrates (including glutamate receptors and MAGUK proteins) (Coultrap and Bayer, 2012). Catalytic activity of CaMKII plays an important role at synapses. For example, CaMKII phosphorylation of the AMPAR subunit GluA1 (on S831) and TARPs regulates hippocampal long-term potentiation (LTP) (Lisman et al., 2012). In addition, a structural role has been proposed for CaMKII (Coultrap and Bayer, 2012; Griffith et al., 2003; Okamoto et al., 2009). For example, the physical binding of CaMKII to GluN2B is involved in synapse maintenance (Figure 4A) (Gambrill and Barria, 2011), and in the recruiting of the proteasome to dendritic spines (Bingol et al., 2010).

Remarkably, GluN2B/CaMKII association is also an important event for memory consolidation. Incubation of acute hippocampal slices with a peptide that inhibits this binding is able to reverse LTP maintenance and decrease synaptic transmission (Sanhueza et al., 2011). In addition, a knockin mouse expressing a GluN2B mutant unable to bind to CaMKII (GluN2B L1298A+R1300Q) displays a reduction in LTP (around 50%) and shows deficits in the early phases of contextual memory consolidation (Halt et al., 2012). However, in contrast with our data and other published reports (Figure 4A) (Gambrill and Barria, 2011; Pi et al., 2010), no change in synapse density or in subcellular localization of GluN2B was observed. Similarly, these knockin mice show normal basal synaptic transmission. These differences may be the result of the acute versus the long-term approaches used to disrupt the GluN2B/CaMKII association. In fact, a recent report shows that, in contrast with WT mice, these knockin animals develop compensatory mechanisms that allow spine outgrowth independent of synaptic activity (Hamilton et al., 2012). It is also important to note that each particular mutation used for disrupting GluN2B/CaMKII binding could potentially produce additional effects that may explain the subtle differences between the studies.

PSDs are highly dynamic structures, able to rapidly respond to changes in synaptic activity with dramatic modifications of their protein content and organization (Ehlers, 2003). However, the precise mechanisms that drive this remodeling remain unknown. Our data suggest that CaMKII acts as a central organizer of excitatory synapses, which works as an activity-dependent scaffold to regulate synaptic NMDARs. The GluN2 content of NMDARs defines many functional properties of the receptors, and GluN2 subunits are differentially regulated. For example, GluN2A is relatively stable at synapses, whereas GluN2B is more mobile and undergoes robust lateral diffusion, internalization, and recycling (Groc et al., 2006; Lavezzari et al., 2004). In addition, subunit composition of synaptic NMDARs is developmentally regulated and changes from predominantly GluN2B-containing to GluN2A-containing during synaptic maturation. We have recently shown that CK2 activity plays a role in this process and that GluN2B S1480 phosphorylation peaks during the critical period for the switch (Sanz-Clemente et al., 2010). The precise role of CaMKII in the NMDAR subunit shift is less clear. For example, incubation of hippocampal slices with the CaMKII inhibitor KN93 does not prevent the LTP-induced NMDAR subunit switch (Matta et al., 2011). However, only a modest percentage (around 40%) of CaMKII is inhibited by 10 μM KN62 (a KN93-analogous drug), in hippocampal slices (Lee et al., 2009). In addition, the pharmacological inhibition of synaptic activity, NMDAR activity or CaMKII activity (using

TTX, APV, or KN93, respectively) does not block GluN2B S1480 phosphorylation, but reduces it by around 50% (Chung et al., 2004; Sanz-Clemente et al., 2010). Data, therefore, are consistent with the constitutively active nature of CK2 and with our model in which GluN2B S1480 phosphorylation is "facilitated" by CaMKII/GluN2B interaction.

In this study, we have identified an unexpected modulator for GluN2B synaptic expression: the physical association between GluN2B and CaMKII. Our data are consistent with a model in which NMDAR-mediated activation of CaMKII leads to the formation of a trimolecular GluN2B/CaMKII/CK2 complex. Therefore, CK2 phosphorylation within the GluN2B PDZ ligand (S1480) is facilitated by the close proximity of the substrate (Figure 4E). Phosphorylation on S1480 results in the disruption of the association of GluN2B with MAGUK proteins and the decrease of the phosphorylation of GluN2B on Y1472, within a neighboring endocytic motif (YEKL). GluN2B-containing receptors diffuse to extrasynaptic sites via a non-PDZ interaction with SAP102 (Chen et al., 2012), where they ultimately will be internalized via the association of the clathrin adaptor complex AP-2 with the GluN2B YEKL motif (Prybylowski et al., 2005; Sanz-Clemente et al., 2010). Therefore, phosphorylation on the PDZ ligand of GluN2B results in a dramatic decrease of synaptic GluN2B expression (Chen et al., 2012). This mechanism controls the clearance of GluN2B from synapses, but does not affect GluN2A subunits, because CaMKII cannot bind to GluN2A (Strack et al., 2000). In addition, the PDZ ligand of GluN2A is not a good substrate for CK2 phosphorylation (Sanz-Clemente et al., 2010). Recent studies support the existence of a significant amount of NMDARs assembled as triheteromers (GluN1/GluN2A/GluN2B) in forebrain (Al-Hallaq et al., 2007; Gray et al., 2011; Rauner and Köhr, 2011). Therefore, triheteromers would be a critical population of synaptic NMDARs at highly plastic synapses (such as CA1 hippocampal neurons) because the presence of GluN2A likely promotes the stable expression of NMDARs at synaptic sites, even if CaMKII is associated with the receptor complex (via the GluN2B subunit). In summary, our data reveal a critical structural role for CaMKII acting as a scaffolding protein to modulate the activity-dependent regulation of synaptic NMDARs.

EXPERIMENTAL PROCEDURES

The use and care of animals used in this study followed the guidelines of the UCSF and NIH Animal Research Advisory Committees. For pull-down and coimmunoprecipitation experiments, samples were lysed in buffer containing 1% Triton X-100 or 1% Triton X-100; 0.5% sodium deoxycholate (DOC); 0.1% SDS in the presence of 1 mM $CaCl_2$; and 3 μM calmodulin (Ca^{2+}/CaM) or 1 mM EGTA (EGTA) and incubated with the appropriate antibody and protein A/G beads or indicated GST-fusion proteins at 4°C. After washes, beads were analyzed by SDS-PAGE and immunoblotting. Immunofluorescence was performed as previously reported (Sanz-Clemente et al., 2010). GFP-tagged GluN2B was transfected into hippocampal neurons at DIV7, and surface expression was analyzed at DIV11–12. The number of synapses was quantified by labeling endogenous PSD-95 and VGlut1 at DIV17 after transfection of pCAG-GluN2B-IRES-GFP at DIV5. For electrophysiological recordings, hippocampi were dissected from P7 *Grin2b*$^{fl/fl}$ mice and biolistically transfected after 2–4 days in culture with pFUGW-Cre:mCherry and either pCAG-GFP or pCAG-GluN2B-IRES-GFP or mutants. Slices were cultured for an additional 14–20 days and dual whole-cell patch-clamp recordings were performed from neighboring CA1 pyramidal cells. NMDAR-EPSCs were recorded at +40 mV in the presence of 10 μM NBQX. Additional details are available in Extended Experimental Procedures.

SUPPLEMENTAL INFORMATION

Supplemental Information includes Extended Experimental Procedures and two figures and can be found with this article online at http://dx.doi.org/10.1016/j.celrep.2013.02.011.

LICENSING INFORMATION

ACKNOWLEDGMENTS

We thank John D. Badger II for technical assistance. We also thank the NINDS sequencing facility and light imaging facility for expertise and advice. This research was supported by the NINDS Intramural Research Program (A.S.-C., K.A.O., and K.W.R.) and grants from the NIMH (J.A.G. and R.A.N.). J.A.G. is funded by a NARSAD Young Investigator Award and is the NARSAD Hammerschlag Family Investigator.

Received: October 25, 2012
Revised: January 18, 2013
Accepted: February 6, 2013
Published: March 7, 2013

REFERENCES

Al-Hallaq, R.A., Conrads, T.P., Veenstra, T.D., and Wenthold, R.J. (2007). NMDA di-heteromeric receptor populations and associated proteins in rat hippocampus. J. Neurosci. *27*, 8334–8343.

Barria, A., and Malinow, R. (2005). NMDA receptor subunit composition controls synaptic plasticity by regulating binding to CaMKII. Neuron *48*, 289–301.

Bayer, K.U., De Koninck, P., Leonard, A.S., Hell, J.W., and Schulman, H. (2001). Interaction with the NMDA receptor locks CaMKII in an active conformation. Nature *411*, 801–805.

Bingol, B., Wang, C.F., Arnott, D., Cheng, D., Peng, J., and Sheng, M. (2010). Autophosphorylated CaMKIIalpha acts as a scaffold to recruit proteasomes to dendritic spines. Cell *140*, 567–578.

Blanquet, P.R. (2000). Casein kinase 2 as a potentially important enzyme in the nervous system. Prog. Neurobiol. *60*, 211–246.

Carmignoto, G., and Vicini, S. (1992). Activity-dependent decrease in NMDA receptor responses during development of the visual cortex. Science *258*, 1007–1011.

Chen, B.S., Gray, J.A., Sanz-Clemente, A., Wei, Z., Thomas, E.V., Nicoll, R.A., and Roche, K.W. (2012). SAP102 mediates synaptic clearance of NMDA receptors. Cell Rep. *2*, 1120–1128.

Chung, H.J., Huang, Y.H., Lau, L.F., and Huganir, R.L. (2004). Regulation of the NMDA receptor complex and trafficking by activity-dependent phosphorylation of the NR2B subunit PDZ ligand. J. Neurosci. *24*, 10248–10259.

Coultrap, S.J., and Bayer, K.U. (2012). CaMKII regulation in information processing and storage. Trends Neurosci. *35*, 607–618.

Cull-Candy, S.G., and Leszkiewicz, D.N. (2004). Role of distinct NMDA receptor subtypes at central synapses. Sci. STKE *255*, re16.

Ehlers, M.D. (2003). Activity level controls postsynaptic composition and signaling via the ubiquitin-proteasome system. Nat. Neurosci. *6*, 231–242.

Gambrill, A.C., and Barria, A. (2011). NMDA receptor subunit composition controls synaptogenesis and synapse stabilization. Proc. Natl. Acad. Sci. USA *108*, 5855–5860.

Gray, J.A., Shi, Y., Usui, H., During, M.J., Sakimura, K., and Nicoll, R.A. (2011). Distinct modes of AMPA receptor suppression at developing synapses by GluN2A and GluN2B: single-cell NMDA receptor subunit deletion in vivo. Neuron *71*, 1085–1101.

Griffith, L.C., Lu, C.S., and Sun, X.X. (2003). CaMKII, an enzyme on the move: regulation of temporospatial localization. Mol. Interv. *3*, 386–403.

Groc, L., Heine, M., Cousins, S.L., Stephenson, F.A., Lounis, B., Cognet, L., and Choquet, D. (2006). NMDA receptor surface mobility depends on NR2A-2B subunits. Proc. Natl. Acad. Sci. USA *103*, 18769–18774.

Groc, L., Bard, L., and Choquet, D. (2009). Surface trafficking of N-methyl-D-aspartate receptors: physiological and pathological perspectives. Neuroscience *158*, 4–18.

Halt, A.R., Dallapiazza, R.F., Zhou, Y., Stein, I.S., Qian, H., Juntti, S., Wojcik, S., Brose, N., Silva, A.J., and Hell, J.W. (2012). CaMKII binding to GluN2B is critical during memory consolidation. EMBO J. *31*, 1203–1216.

Hamilton, A.M., Oh, W.C., Vega-Ramirez, H., Stein, I.S., Hell, J.W., Patrick, G.N., and Zito, K. (2012). Activity-dependent growth of new dendritic spines is regulated by the proteasome. Neuron *74*, 1023–1030.

Hathaway, G.M., and Traugh, J.A. (1982). Casein kinases—multipotential protein kinases. Curr. Top. Cell. Regul. *21*, 101–127.

Ippolito, D.M., and Eroglu, C. (2010). Quantifying synapses: an immunocytochemistry-based assay to quantify synapse number. J. Vis. Exp., doi: 2210.3791/2270.

Lau, C.G., and Zukin, R.S. (2007). NMDA receptor trafficking in synaptic plasticity and neuropsychiatric disorders. Nat. Rev. Neurosci. *8*, 413–426.

Lavezzari, G., McCallum, J., Dewey, C.M., and Roche, K.W. (2004). Subunit-specific regulation of NMDA receptor endocytosis. J. Neurosci. *24*, 6383–6391.

Lee, S.J., Escobedo-Lozoya, Y., Szatmari, E.M., and Yasuda, R. (2009). Activation of CaMKII in single dendritic spines during long-term potentiation. Nature *458*, 299–304.

Lisman, J., Yasuda, R., and Raghavachari, S. (2012). Mechanisms of CaMKII action in long-term potentiation. Nat. Rev. Neurosci. *13*, 169–182.

Litchfield, D.W. (2003). Protein kinase CK2: structure, regulation and role in cellular decisions of life and death. Biochem. J. *369*, 1–15.

Matta, J.A., Ashby, M.C., Sanz-Clemente, A., Roche, K.W., and Isaac, J.T. (2011). mGluR5 and NMDA receptors drive the experience- and activity-dependent NMDA receptor NR2B to NR2A subunit switch. Neuron *70*, 339–351.

Merrill, M.A., Chen, Y., Strack, S., and Hell, J.W. (2005). Activity-driven postsynaptic translocation of CaMKII. Trends Pharmacol. Sci. *26*, 645–653.

O'Leary, H., Liu, W.H., Rorabaugh, J.M., Coultrap, S.J., and Bayer, K.U. (2011). Nucleotides and phosphorylation bi-directionally modulate Ca2+/calmodulin-dependent protein kinase II (CaMKII) binding to the N-methyl-D-aspartate (NMDA) receptor subunit GluN2B. J. Biol. Chem. *286*, 31272–31281.

Okamoto, K., Bosch, M., and Hayashi, Y. (2009). The roles of CaMKII and F-actin in the structural plasticity of dendritic spines: a potential molecular identity of a synaptic tag? Physiology (Bethesda) *24*, 357–366.

Olsten, M.E., and Litchfield, D.W. (2004). Order or chaos? An evaluation of the regulation of protein kinase CK2. Biochem. Cell Biol. *82*, 681–693.

Omkumar, R.V., Kiely, M.J., Rosenstein, A.J., Min, K.T., and Kennedy, M.B. (1996). Identification of a phosphorylation site for calcium/calmodulindependent protein kinase II in the NR2B subunit of the N-methyl-D-aspartate receptor. J. Biol. Chem. *271*, 31670–31678.

Pi, H.J., Otmakhov, N., El Gaamouch, F., Lemelin, D., De Koninck, P., and Lisman, J. (2010). CaMKII control of spine size and synaptic strength: role of phosphorylation states and nonenzymatic action. Proc. Natl. Acad. Sci. USA *107*, 14437–14442.

Prybylowski, K., Chang, K., Sans, N., Kan, L., Vicini, S., and Wenthold, R.J. (2005). The synaptic localization of NR2B-containing NMDA receptors is controlled by interactions with PDZ proteins and AP-2. Neuron *47*, 845–857.

Quinlan, E.M., Olstein, D.H., and Bear, M.F. (1999). Bidirectional, experience-dependent regulation of N-methyl-D-aspartate receptor subunit composition in the rat visual cortex during postnatal development. Proc. Natl. Acad. Sci. USA *96*, 12876–12880.

Rauner, C., and Köhr, G. (2011). Triheteromeric NR1/NR2A/NR2B receptors constitute the major N-methyl-D-aspartate receptor population in adult hippocampal synapses. J. Biol. Chem. *286*, 7558–7566.

Sanhueza, M., Fernandez-Villalobos, G., Stein, I.S., Kasumova, G., Zhang, P., Bayer, K.U., Otmakhov, N., Hell, J.W., and Lisman, J. (2011). Role of the CaMKII/NMDA receptor complex in the maintenance of synaptic strength. J. Neurosci. *31*, 9170–9178.

Sanz-Clemente, A., Matta, J.A., Isaac, J.T., and Roche, K.W. (2010). Casein kinase 2 regulates the NR2 subunit composition of synaptic NMDA receptors. Neuron *67*, 984–996.

Sanz-Clemente, A., Nicoll, R.A., and Roche, K.W. (2013). Diversity in NMDA receptor composition: many regulators, many consequences. Neuroscientist *19*, 62–75.

Strack, S., McNeill, R.B., and Colbran, R.J. (2000). Mechanism and regulation of calcium/calmodulin-dependent protein kinase II targeting to the NR2B subunit of the N-methyl-D-aspartate receptor. J. Biol. Chem. *275*, 23798–23806.

Traynelis, S.F., Wollmuth, L.P., McBain, C.J., Menniti, F.S., Vance, K.M., Ogden, K.K., Hansen, K.B., Yuan, H., Myers, S.J., and Dingledine, R. (2010). Glutamate receptor ion channels: structure, regulation, and function. Pharmacol. Rev. *62*, 405–496.

Cell PRESS
Open ACCESS

EXTENDED EXPERIMENTAL PROCEDURES

Neuronal Cultures, Antibodies, and Reagents

Primary cultured neurons (cortical or hippocampal) were prepared from E18 Sprague-Dawley rats as previously described (Roche and Huganir, 1995). The use and care of animals used in this study followed the guidelines of the NIH Animal Research Advisory Committee. We obtained the utilized antibodies from Thermo Scientific [phosphorylation state-specific S1480 GluN2B (PA1-4733), CaMKII (MA1-048)], Sigma [GluN2B (M-265), CaMKII (C6974), CK2beta (C3617)], Millipore [CK2beta (04-1128), VGlut1 (AB5905)], AffinityBioReagents [PSD-95 (MA1-046)], Bethyl Laboratory [GST (A190-122A)] and Invitrogen [GFP (A11122), Alexa-secondary antibodies). Calmodulin was purchased from Millipore; all other drugs and reagents from Tocris.

HEK293T Transfection, Pull-Down Assays, and Coimmunoprecipitation

HEK293T cells were transfected using Lipofectamine 2000 as previously described (Lussier et al., 2005). For analysis of GluN2B S1480 phosphorylation we transfected PSD-95, GluN1 and GluN2B (ratio 1:5:10) and cells were maintained in 100 μM APV; 20 mM $MgCl_2$ to avoid excitotoxicity. For pull-down experiments, transfected HEK293T cells were lysed in IP buffer (50 mM PIPES pH: 7.5; 150 mM NaCl) containing 1% Triton X-100 in the presence of either 1 mM $CaCl_2$ and 3 μM calmodulin (Ca/CaM) or 1 mM EGTA (EGTA) (Bayer et al., 2001). Lysates were centrifuged at 20,000 g for 15 min. and supernatant incubated for 1 hr at 4°C with GST-GluN2B C-terminal (residues 1120-1482) pre-blocked with 3% NGS in PBS. After three washes with RIPA-IP buffer (IP buffer containing 1% TX-100; 0.5% DOC and 0.1% SDS) beads were subjected to SDS-PAGE and immunoblotted for the indicated antibodies. For co-immunoprecipitation experiments, cortical neurons or tranfected HEK293T cells were lysed in RIPA-IP buffer with Ca/CaM. After the removal of insoluble complexes by centrifugation at 100,000 g for 30 min at 4°C, supernatant was incubated with the indicated antibodies and protein G-Sepharose beads at 4°C overnight. Samples were immunoblotted after 3x15 min washed in RIPA-IP buffer.

Immunofluorescence

Receptor surface expression was analyzed as previously described (Sanz-Clemente et al., 2010). Briefly, hippocampal neurons were transfected at DIV7 with GFP-tagged GluN2B (WT or mutants) and surface-expressed receptors were labeled with anti-GFP antibody for 15 min at RT at DIV11–12. After washes and fixation with 4% PFA in PBS containing 4% sucrose, cells were labeled with Alexa 555-conjugated secondary antibody (shown in white for clarity). The intracellular pool of receptors was identified by permeabilizing cells with 0.25% TX-100 and labeling with anti-GFP and Alexa 633-conjugated secondary antibodies (shown in green). Cells were imaged on a Zeiss LSM 510 confocal microscope. Serial optical sections collected at 0.35 μm intervals were used to create maximum projection images. Quantification was performed analyzing the fluorescence intensity of 3-4 independent areas per neuron using MetaMorph 6.0 software (Universal Imaging Corp) and it is presented as ratio surface/intracellular intensities (mean ±SEM).

For quantification of the number of synapses, hippocampal neurons were transfected at DIV5 with pCAG-GluN2B-IRES-GFP. At DIV17 cells were fixed and permeabilized as above and endogenous PSD-95 and VGlut1 labeled by incubation with specific primary antibodies and Alexa 555- and 633-conjugated secondary antibodies. A synapse is defined as a co-localized VGlut1 and PSD-95 puncta (Ippolito and Eroglu, 2010). The number of co-localized puncta in GFP-expressing neurons (3-4 regions of 30 μm/cell) was quantified using MetaMorph 6.0.

Electrophysiology in Organotypic Slice Cultures

Single-floxed GluN2B (*Grin2b*$^{fl/fl}$) or double-floxed GluN2AGluN2B (*Grin2a*$^{fl/fl}$*Grin2b*$^{fl/fl}$) mice were generated as previously described (Akashi et al., 2009; Gray et al., 2011; Mishina and Sakimura, 2007), and were housed according to the IACUC guidelines at the University of California, San Francisco. Cultured slices were prepared and transfected as previously described (Schnell et al., 2002). Briefly, hippocampi were dissected from P7 WT *Grin2b*$^{fl/fl}$ or *Grin2a*$^{fl/fl}$*Grin2b*$^{fl/fl}$ mice and biolistically co-transfected after 2-4 days in culture with pFUGW-Cre:mCherry (expressing a nuclear targeted Cre:mCherry fusion protein) and either pCAGGS-GFP or pCAGGS-GluN2B-IRES-GFP (with WT or mutant mouse GluN2B). Slices were cultured for an additional 14–20 days before recording. Slices were recorded in a submersion chamber on an upright Olympus microscope, perfused in room temperature normal ACSF saturated with 95% O_2/5% CO_2. Picrotoxin (0.1 mM) and NBQX (10 μM) were added to the ACSF to block $GABA_A$ and AMPA receptors respectively. CA1 pyramidal cells were visualized by infrared differential interference contrast microscopy and transfected neurons were identified by epifluorescence microscopy. The intracellular solution contained (in mM) CsMeSO4 135, NaCl 8, HEPES 10, Na-GTP 0.3, Mg-ATP 4, EGTA 0.3, and QX-314 5. Cells were recorded with 3 to 5MΩ borosilicate glass pipettes, following stimulation of Schaffer collaterals with bipolar placed in stratum radiatum of the CA1 region. Series resistance was monitored and not compensated, and cells in which series resistance varied by 25% during a recording session were discarded. Synaptic responses were collected with a Multiclamp 700B amplifier (Axon Instruments, Foster City, CA), filtered at 2 kHz, digitized at 10 Hz. All paired recordings involved simultaneous whole-cell recordings from transfected neuron and a neighboring untransfected neuron. NMDAR-EPSCs were recorded at +40 mV in the presence of 10 μM NBQX. The stimulus was adjusted to evoke a measurable, monosynaptic EPSC in both cells. Paired amplitude data were analyzed with a Wilcoxon signed-rank test and the paired decay kinetics were

analyzed with a two-tailed paired Student's t test. Comparison of paired data groups were performed using a Mann-Whitney U test. Linear regressions were obtained using the least-squares method. All errors bars represent standard error measurement.

SUPPLEMENTAL REFERENCES

Akashi, K., Kakizaki, T., Kamiya, H., Fukaya, M., Yamasaki, M., Abe, M., Natsume, R., Watanabe, M., and Sakimura, K. (2009). NMDA receptor GluN2B (GluR epsilon 2/NR2B) subunit is crucial for channel function, postsynaptic macromolecular organization, and actin cytoskeleton at hippocampal CA3 synapses. J. Neurosci. *29*, 10869–10882.

Lussier, M.P., Cayouette, S., Lepage, P.K., Bernier, C.L., Francoeur, N., St-Hilaire, M., Pinard, M., and Boulay, G. (2005). MxA, a member of the dynamin superfamily, interacts with the ankyrin-like repeat domain of TRPC. J. Biol. Chem. *280*, 19393–19400.

Mishina, M., and Sakimura, K. (2007). Conditional gene targeting on the pure C57BL/6 genetic background. Neurosci. Res. *58*, 105–112.

Roche, K.W., and Huganir, R.L. (1995). Synaptic expression of the high-affinity kainate receptor subunit KA2 in hippocampal cultures. Neuroscience *69*, 383–393.

Schnell, E., Sizemore, M., Karimzadegan, S., Chen, L., Bredt, D.S., and Nicoll, R.A. (2002). Direct interactions between PSD-95 and stargazin control synaptic AMPA receptor number. Proc. Natl. Acad. Sci. USA *99*, 13902–13907.

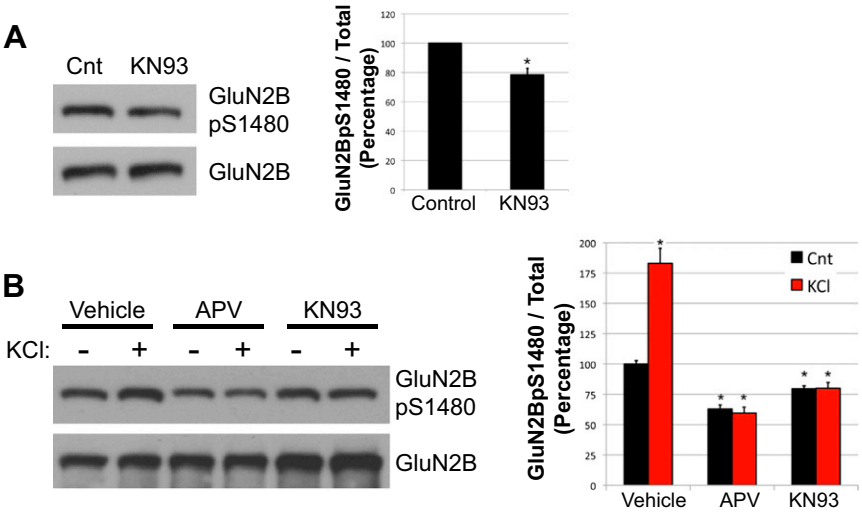

Figure S1. CaMKII Regulates CK2-Mediated Phosphorylation of GluN2B S1480, Related to Figure 1

(A) Cortical neurons (DIV10-12) were incubated with 1 μM KN-93 for 1 hr to block CaMKII activity. Total membrane fraction was isolated as previously described (Sanz-Clemente et al., 2010) and samples were immunoblotted with a GluN2B S1480 phosphorylation state-specific antibody. Membrane was reblotted against GluN2B to obtain ratio of S1480 phosphorylation. Graph represents mean ±SEM. *$p < 0.05$ in a Wilcoxon test. $n = 6$.

(B) Cortical neurons were pre-treated with 100 μM APV (overnight) or 5 μM KN93 (1 hr) and incubated with 20 mM KCl for 5 min to induce neuronal depolarization. Total membranes were isolated as before and level of GluN2B S1480 analyzed by immunoblotting. Graph represents mean ±SEM. *$p < 0.05$ in a Wilcoxon test. $n = 3$.

Cell PRESS
Open ACCESS

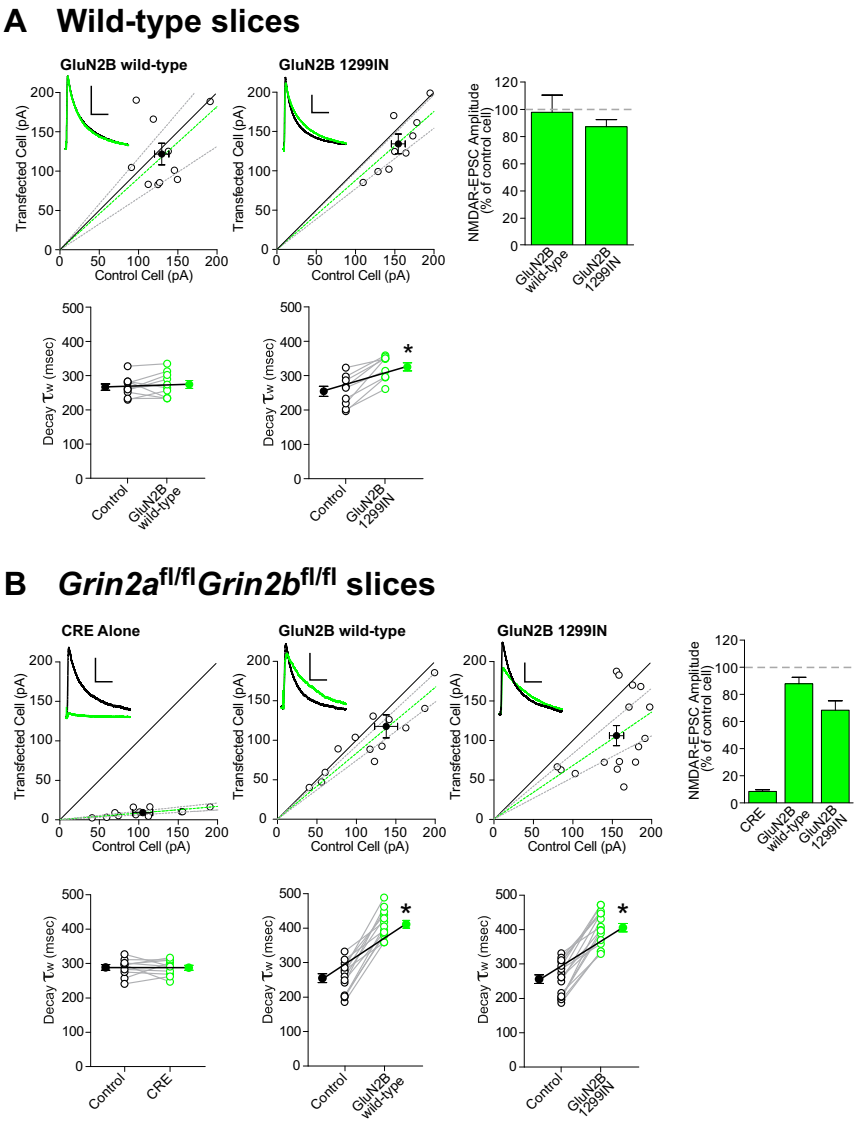

Figure S2. Disrupting the GluN2B-CaMKII Interaction Increases GluN2B Synaptic Content without Affecting GluN2B Gating Properties, Related to Figure 4

(A and B) Organotypic hippocampal slice cultures were made from P7 wild-type (A) or *Grin2a*$^{fl/fl}$*Grin2b*$^{fl/fl}$ (B) mice, biolistically transfected with GluN2B mutants and/or CRE on DIV2-4, and paired whole-cell recordings were obtained from transfected and neighboring CA1 pyramidal neurons on DIV18-24.

(A) Overexpression in wild-type slices. Scatter plots of peak amplitudes of NMDAR-EPSCs from single pairs (open circles) and mean ±SEM (filled circles) from transfected and control cells (top, mean amplitude (pA): left, GluN2B wild-type, control 129.6 ± 9.2, transfected 121.7 ± 13.8, n = 10; right, GluN2B 1299IN, control 154.5 ± 8.8, transfected 134.3 ± 12.5, n = 9). Dashed lines represent linear regression and 95% confidence interval. Sample traces are as follows: control cell, black; transfected cell, green; scale bars represent 300 ms and 50 pA. Bar graph represents the mean ±SEM of the ratios of the NMDAR-EPSC amplitudes from transfected and control cells from each pair, expressed as percentages (GluN2B wild-type 97.7 ± 13.5, n = 10; GluN2B 1299IN 86.0 ± 4.7, n = 9). Bottom, NMDAR-EPSC decay times from cell pairs expressed in ms as a weighted tau (τ_w) from paired transfected and control cells (mean decay, ms: left, GluN2B wild-type, control 268.7 ± 12.0, transfected 274.6 ± 12.3, n = 10, p = 0.36; right, GluN2B 1299IN, control 254.6 ± 14.8, transfected 327.3 ± 12.5, n = 9, p < 0.0001). Decay kinetics were analyzed by a paired Student's t test, *p < 0.0001.

(B) Molecular replacement in slices from *Grin2a*$^{fl/fl}$*Grin2b*$^{fl/fl}$ mice. Scatter plots of peak amplitudes of NMDAR-EPSCs from single pairs (open circles) and mean ±SEM (filled circles) from transfected and control cells (top, mean amplitude (pA): left, Cre alone, control 105.1 ± 12.6, transfected 9.0 ± 1.5, n = 12; center, GluN2B wild-type, control 137.4 ± 14.6, transfected 117.1 ± 14.5, n = 13; right, GluN2B 1299IN, control 155.5 ± 9.1, transfected 105.6 ± 12.7, n = 16). Dashed lines represent linear regression and 95% confidence interval. Sample traces are as follows: control cell, black; transfected cell, green; scale bars represent 300 msec and 50 pA. Bar graph represents the mean ±SEM of the ratios of the NMDAR-EPSC amplitudes from transfected and control cells from each pair, expressed as percentages (Cre alone 8.5 ± 1.2, n = 12; GluN2B wild-type 87.9 ± 4.7, n = 13; GluN2B 1299IN 68.3 ± 7.0, n = 16). Bottom, NMDAR-EPSC decay times from cell pairs expressed in msec as a weighted tau (τ_w) from paired transfected and control cells (mean decay, msec: left, Cre alone, control 271.3 ± 8.0, transfected 269.8 ± 7.3, n = 10, p = 0.82; center, GluN2B wild-type, control 256.4 ± 13.0, transfected 413.8 ± 11.2, n = 13, p < 0.0001; right, GluN2B 1299IN, control 256.3 ± 12.4, transfected 406.2 ± 12.3, n = 16, p < 0.0001). Decay kinetics were analyzed by a paired Student's t test, *p < 0.0001.